Available online at www.sciencedirect.com

ScienceDirect

Procedia Engineering 10 (2011) 3628–3635

Engineering Procedia

ICM11

Characterization of the behavior of a turbine rotor steel by inverse analysis on the small punch test

S. Foletti[a]*, M. Madia[a], A. Cammi[b], G. Torsello[b]

[a]*Politecnico di Milano, via La Masa 1, Milano 20156, Italy*
[b]*RSE SpA, via Rubattino 54, Milano 20134, Italy*

Abstract

The present work focuses on the application of the inverse methods on the small punch test (SPT) in order to predict the behavior of turbine rotor steel upon in-service loading. A numerical framework has been implemented in which the small punch test has been simulated by means of finite element analyses and compared with the experimental results in order to assess the material parameters. The comparison has been carried out relying on the load-displacement curve of the SPT. The material behavior has been represented through an elastic-plastic constitutive law and a micro-mechanical damage model to account for softening and material failure. The assessed material parameters have been employed in the simulation of the tensile test, showing a good approximation of the basic mechanical properties of the material.

Keywords: small punch test; FEA; GTN model; inverse analysis

1. Introduction

The possibility to monitor the degradation of the material properties by means of non-destructive methods received an increasing attention in the last decade. The important goal is to estimate the residual life of a component and hold it in-service beyond its designed life.

The non-destructive techniques have the great advantage to evaluate the material properties in-situ, in particular the small punch test shows to be very attractive and promising as it relies on a small, but

* Corresponding author. Tel.: +39-02-2399-8629; fax: +39-02-2399-8263.
E-mail address: stefano.foletti@polimi.it.

 doi:10.1016/j.proeng.2011.04.597

representative material volume of the component in-service [1,2] and it has been successfully applied in other research fields [3-7].

The present work deals with recent developments of an activity devoted to the characterization of the tensile and fracture properties of steel grades commonly employed in the construction of high- and mid-pressure turbine rotors [8]. The attention has been focused on the development of a robust numerical frame for the assessment of the material parameters characterizing the elastic-plastic constitutive law and the micro-mechanical damage model (the well-known GTN model, [9,10]). The model relies on a set of well-established experimental test (SPT, monotonic tensile tests), on finite element simulations of the experimental tests and on a minimization tool which has been developed within the present research. Starting from the calibration of the material parameters by the simulation of the SPT load displacement curve, the basic mechanical properties of the material investigated have been predicted with a satisfactory approximation.

2. Experimental tests

The material under investigation is a 3.5NiCrMoV steel and two different kind of experimental tests have been performed: small punch tests in order to estimate the load displacement curve and tensile tests to assess the basic mechanical properties.

2.1. The small punch test

The schematic of the small punch test is showed in Fig 1.a: the specimen is a small disc which is clamped in a die by means of a down-holder. The die has a central bore in which the puncher can slide, here a puncher with spherical head is used. The tests have been carried out at room temperature.

The load displacement curves for two different specimens are given in Fig 1.b. It is extremely important to notice the very good reproducibility of the test, as it is the basis of the inverse analysis.

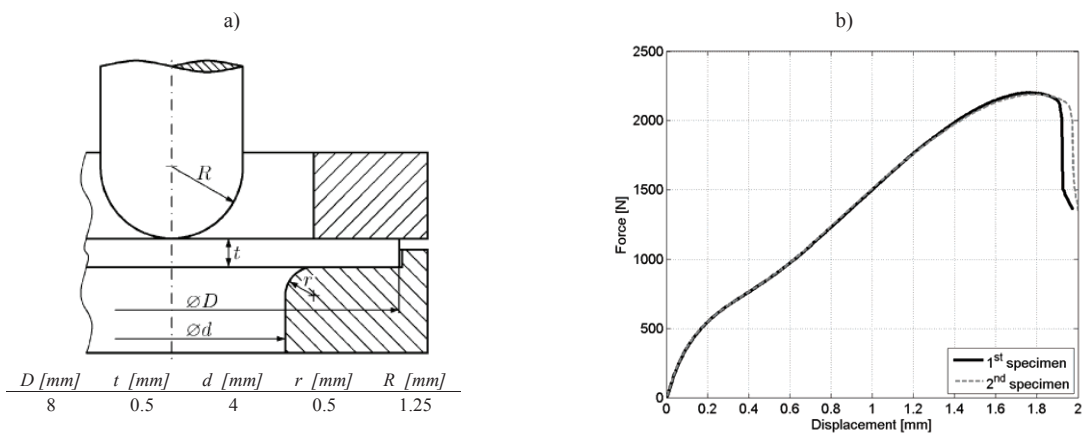

Fig. 1. SPT: a) schematic of the test device; b) load-displacement curve.

2.2. Tensile tests

Tensile tests have been performed at room temperature on standard smooth specimens characterised by a diameter of 5 mm. The axial elongation has been measured by an extensometer with a gauge length of 25 mm. The yield strength of the material is 770 MPa, whereas the tensile strength is 885 MPa.

Another experimental test has been conducted in order to obtain the true stress–true plastic strain curve (yield curve) on standard smooth specimens characterised by a diameter of 10 mm. The axial elongation has been measured using an extensometer with a gauge length of 50 mm while the transverse elongation has been measured by a diametral extensometer to determine the strain values beyond necking. The true stress–true plastic strain curve is reported in Fig 3.

3. Numerical model

The numerical model has been implemented using the general purpose finite element code ABAQUS [11]. The Explicit solver has been used for the analysis in order to account for the failure of the material. As the purpose of the numerical model is to simulate the small punch test and the tensile test, axisymmetric models have been used.

The most important part in this kind of analyses is to choose the proper material model in order to simulate properly the material behavior. The most of the effort has been spent in finding the right definition of the elastic-plastic constitutive law, whereas for the micro-mechanical damage model the Gurson-Tvergaard-Needleman (GTN) model implemented in ABAQUS/Explicit has been used [9,10].

As the commonly employed hardening laws tend to be less accurate at large plastic strain, a bilinear function with four parameters has been used to approximate the elastic-plastic behaviour [12]:

$$\sigma = \begin{cases} \sigma_0 + K_1 \varepsilon_{pl} & 0 \le \varepsilon_{pl} \le \varepsilon_u \\ \sigma_u + K_2 \left(\varepsilon_{pl} - \varepsilon_u \right) & \varepsilon_u \le \varepsilon_{pl} \le \varepsilon_{\max} \end{cases} \tag{1}$$

where:

$$\begin{cases} K_1 = \dfrac{\sigma_u - \sigma_0}{\varepsilon_u} \\ K_2 = \dfrac{\sigma_{\max} - \sigma_u}{\varepsilon_{\max} - \varepsilon_u} \end{cases} \tag{2}$$

in which σ_0, σ_u, ε_u and σ_{max} represent the initial yield stress, the uniform yield stress, the uniform plastic strain and the yield stress at plastic strain ε_{max} (here fixed to ε_{max} = 1 mm/mm), respectively.

About the GTN model, the formulation implemented in ABAQUS/Explicit allows for failure, thus the yield surface can be expressed in the following form:

$$\Phi = \left(\frac{\sigma_{eq}}{\sigma_y} \right)^2 + 2 \cdot q_1 \cdot f^* \cdot \cosh\left(-\frac{3}{2} \cdot \frac{q_2 \cdot p}{\sigma_y} \right) - \left(1 + q_3 f^{*2} \right) = 0 \tag{3}$$

in which σ_{eq} is the equivalent von Mises stress, p is the hydrostatic pressure, σ_y is the yield strength of the metal matrix, q_i are dimensionless coefficients and f^* is the function accounting for the loss of stress carrying capacity due to the presence and coalescence of voids:

$$f^* = \begin{cases} f & \text{if } f \le f_c \\ f_c + \dfrac{\overline{f}_F - f_c}{f_F - f_c} \cdot (f - f_c) & \text{if } f_c < f < f_F \\ \overline{f}_F & \text{if } f \ge f_F \end{cases} \quad (4)$$

in which f_c is the critical void volume fraction and f_F is the value at which the complete failure occurs. There exists also an evolution law accounting for growth ($\dot{f}_{gr}$) and nucleation ($\dot{f}_{nucl}$) of voids within the material:

$$\dot{f} = \dot{f}_{gr} + \dot{f}_{nucl} \quad (5)$$

Regarding the finite element mesh, linear elements with reduced integration have been used for all the models. Moreover the puncher and the die have been modelled as rigid surfaces and a penalty contact formulation has been used for the interaction among the parts.

4. Inverse analysis

4.1. Calibration of the material parameters

The inverse analysis applied to the SPT can be regarded as a powerful tool in order to predict the basic mechanical properties, as well as the fracture properties of the material. The main issue is given by the calibration of the material parameters (Eq 1 to 5) through the simulation of the small punch test. In particular the calibration has been performed by splitting the LDC in different regions (Fig 2): the parameters for the elastic-plastic law has been identified using the regions I and II, whereas the GTN model has been calibrated taking into account the other regions, in which the nucleation and growth of voids occurs and damage localises up to the final fracture.

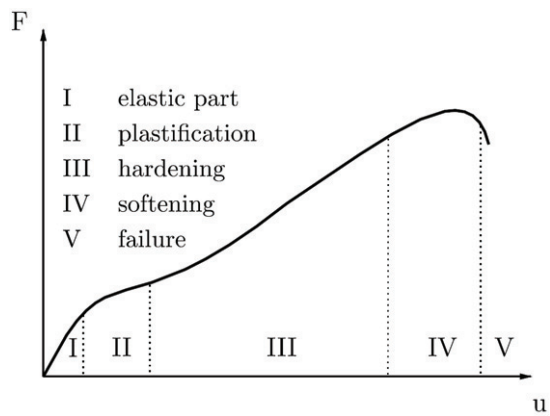

Fig. 2. Inverse analysis: subdivision of the LDC [12].

The computational frame has been built using the commercial software ABAQUS and MATLAB [13], which have been linked by a FORTRAN subroutine in order to realize an automatic iterative method.

Given a starting set of material parameters, a multidimensional nonlinear minimization algorithm has been used to minimize the following function:

$$err = \sqrt{\sum_{i=1}^{N}\left(F_i^{calc} - F_i^{\exp}\right)^2} \tag{6}$$

in which N is the number of points considered in the optimisation, F_i^{calc} is the force value calculated by finite element analyses and $F_i^{\exp}$ is the force value from the experimental small punch test.

As already observed by Linse et al, [12], the LDC of the SPT does not provide enough information for a unique determination of the hardening parameters, i.e. different yield curves provide the same LDC. The identified hardening parameters can be strongly affected by the initial set used in the iterative method. In order to overcome this problem 10 sets of initials paramenters, [σ_0 σ_u ε_u σ_{max}], have been randomly extracted from a given interval (parameters space), see Tab 1.

The results reported in Fig 3 and Tab 1 in terms of both mean value and standard deviation, show that the mean values remain close to the experimental ones.

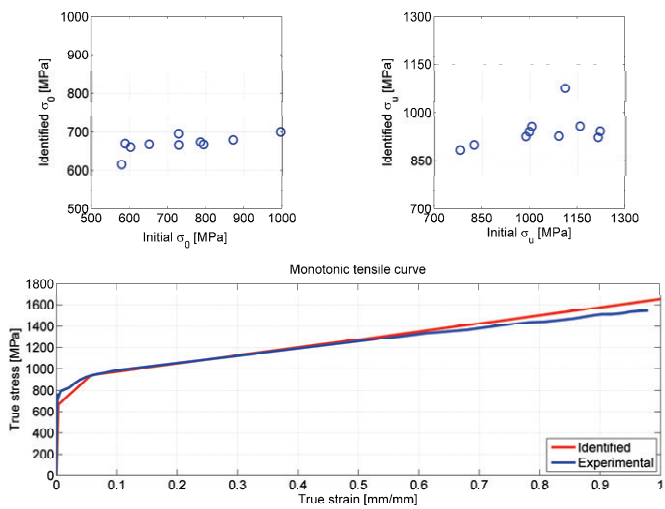

Fig. 3. Inverse analysis: identification of the metal matrix constitutive law.

Table 1. Identified hardening parameters.

Parameters	*Parameters space*	*Experimental value*	*Identified mean value*	*Standard deviation*	*Error [%]*
σ_0 [MPa]	[500, 1000]	773	670	21.9	-13.3
σ_u [MPa]	[650, 1200]	942	944	49.4	+0.2
ε_u [mm/mm]	[0.03, 0.07]	0.0537	0.0538	0.0104	+0.2
σ_{max} [MPa]	[1000, 2000]	1537	1657	297.4	+7.8

All the material parameters have been calculated via the foregoing iterative method, but the critical void volume fraction (f_c) and the void volume fraction at failure (f_F). The critical void volume fraction has been identified from the finite element analysis, considering the trend of the void volume fraction in the element in which failure occurs [14]. In particular f_c is the void volume fraction evaluated for the punch displacement at which the simulated and the experimental curve start diverging (initiation of void coalescence). The value of f_F has been determined as the one giving the best fit of the region V of the experimental LDC (see Fig 2).
The identified material parameters have been reported in Tab 2. The results of the calibration in terms of LDC are depicted in Fig 4. The simulated curve represents a fairly good approximation of the experimental one, there is just a slight discrepancy in region III.

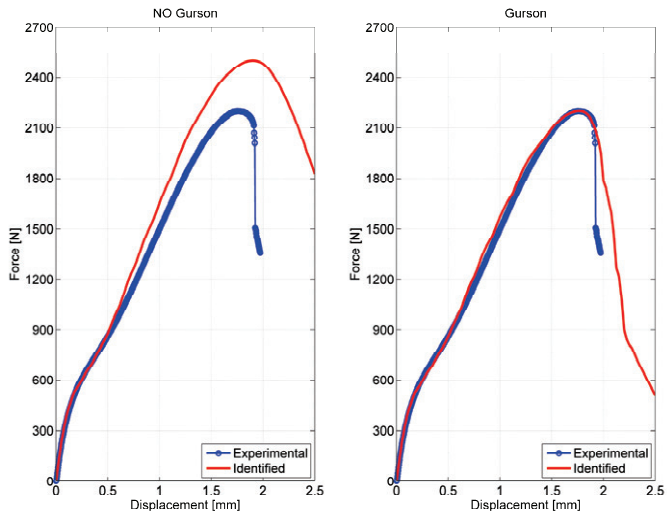

Fig. 4. Inverse analysis: identification of GTN model parameters.

Table 2. Identified GTN model parameters.

Parameters	q_1	ε_n	f_n	f_c	f_F
Identified values	1.165	0.12	0.07	0.185	0.28

4.2. Prediction of the basic mechanical properties

The parameters given in Tab 1 and Tab 2 have been used in the simulation of the tensile test in order to predict the basic mechanical properties of the material by means of a FE model. The resulting curve is given in Fig 5 and compared with the experimental one. The predicted curve yields a low value of the yield strength, but it provides good estimations for the tensile strength and the elongation at fracture.

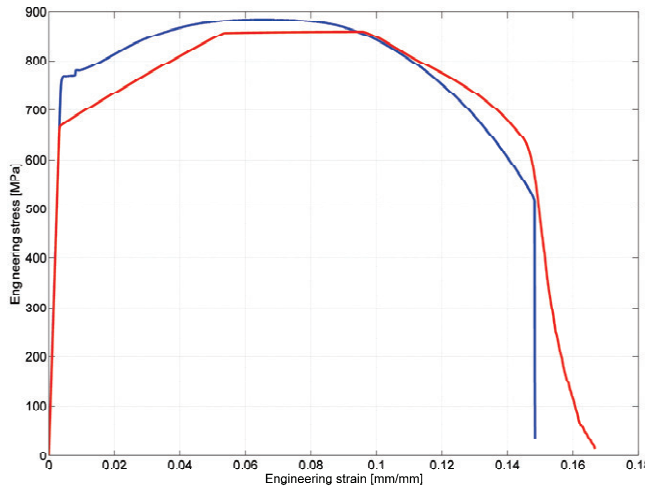

Fig. 5. Comparison between experimental and simulated tensile test.

5. Concluding remarks

The work focused on the characterization of a turbine rotor steel by inverse analysis on small punch test. Both experimental work and numerical simulations have been carried out in order to build a numerical frame based on inverse analysis for the prediction of the basic mechanical properties of the material under investigation.

The material modelling relied on a proper elastic-plastic constitutive law simulating the behaviour of the material matrix and on the GTN model accounting for softening and final fracture of the material.

The calibration of the material parameters provided a satisfactory approximation of the experimental load displacement curve, a slight discrepancy occurred just in the region III of the LDC.

The identified material, applied to the tensile test, yielded a general good estimation of the material behaviour. Further activities will deal with the prediction of the fracture properties for the investigated material.

Acknowledgements

This work has been financed by the Research Fund for the Italian Electrical System under the Contract Agreement between ERSE (now RSE SpA) and the Ministry of Economic Development – General Directorate for Nuclear Energy, Renewable Energy and Energy Efficiency stipulated on July 29, 2009 in compliance with the Decree of March 19, 2009.

References

[1] Small Punch Test Method for Metallic Materials. Part A: A Code of Practice for Small Punch Creep Testing. Part B: A Code of Practice for Small Punch Testing for Tensile and Fracture Behavior. Documents of CEN WS21, Brussels (in press).
[2] Lucas GE. Review of small specimen test technique for irradiation testing. *Metall. Trans.* 21A 1990; 1105–1119.
[3] Ishii T, Ohmi M, Saito J, Hoshiya T, Ooka N, Jitsukawa S. Development of a small specimen test machine to evaluate irradiation embrittlement of fusion reactor materials. *J. Nucl. Mater.* 2000; 1023–1027.

[4] Song SH, Faulkner RG, Flewitt PEJ, Marmy P, Weng LQ. Small punch test evaluation of neutron-irradiation-induced embrittlement of a Cr–Mo low-alloy steel. *Mater. Charact.* 2004; 53(1):35–41.
[5] Bulloch JH. A review of the ESB small punch test data on various plant components with special emphasis on fractographic details. *Eng. Fail. Anal.* 2002; 9(5):11–34.
[6] Kurtz SM, Jewett CW, Bergström JS, Foulds JR, Edidin AA. Miniature specimen shear punch test for UHMWPE used in total joint replacements. *Biomaterials* 2002; 23:1907–1919.
[7] Baik JM, Kameda J, Buck O. Small punch test evaluation of intergranular embrittlement of an alloy steel. *Scr. Metall.* 1983; 17(12):1443–1447.
[8] Foletti S, Madia M, Cammi A, Torsello G. Characterization of the fracture behaviour of a turbine rotor steel by means of the small punch test. *European Conference on Fracture (ECF18)* 2010, Dresden, Germany.
[9] Tvergaard V. Influence of voids on shear band instabilities under plane strain conditions. *Int. J. Fracture Mech.* 1981; 17(4):389–407.
[10] Tvergaard V, Needleman A. Analysis of the cup-cone fracture in a round tensile bar. *Acta Metall.* 1984; 32(1):157–169.
[11] ABAQUS, v.6.9-1. ABAQUS reference manuals. 2009.
[12] T. Linse, M. Kuna, J. Schuhknecht, H.-W. Viehrig. Usage of the small-punch-test for the characterisation of reactor vessel steels in the brittle–ductile transition region *Engineering Fracture Mechanics* 75 (2008) 3520–3533.
[13] MATLAB v. R2007b. The Mathworks inc. 2007.
[14] Cuesta II, Alegre JM, Lacalle R. Determination of the Gurson-Tvergaard damage model parameters for simulating small punch tests. *Fatigue Fract Engng Mater Struct* 2010; 33:703-713.